P

ARI

Custom Search | BASIC Search | List

*DoD SBIR / STTR*

# *DETAILS - Awards Search Results*

**Program:** SBIR

**Agency:** AF

**Field Office:** TTOAEDC

**TOPIC Number:** AF97-248

**Control Number:** 97TTO-253

**Contract Number:** F40600-97-C-0009

**Phase:** 1

**Awarded In:** 97

**Award Amount:** $99,863

**Award Start Date:** 07MAY97

**Award Completion Date:** 07FEB98

**Proposal Title:** Optical Instrument to Measure the Mass Concentration and Size Distribution of Smoke Particles

**Principal Investigator Name:** Cecil F. Hess, PhD

**Principal Investigator Phone:** 714-553-0688

## Firm

METROLASER, INC.
18006 Skypark Circle #108
Irvine, CA 92614

**Woman Owned:** N
**Minority Owned:** Y
**Number of Employees:** 30

**Keywords:** MASS FRACTION OPTICAL DIAGNOSTICS SOOT PARTICLES SIZING

**Abstract:** This proposal describes the development of a system to measure in-situ and in real-time, the size distribution and mass concentration of soot particles in turbojet exhausts. The proposed system will work in-situ in highly turbulent environments. The total signal will yield soot mass concentration while the time-resolved signal will yield particle size. Its potentially compact size and large dynamic measurement range will give the system broad market potential in a variety of industries attempting to measure and suppress particle pollution. The Phase I work will include developing an analytical model to derive soot mass concentration and particle size from the signal. A breadboard will be built to conduct proof-of-concept experiments, and the preliminary design for a field system will be produced. The proposed system will be particularly valuable to the Air Force to measure soot in engine test facilities which are characterized by high vibration and noise levels.

AEDC-TR-97-

# OPTICAL INSTRUMENT TO MEASURE THE MASS CONCENTRATION AND SIZE DISTRIBUTION OF SMOKE PARTICLES

S.R. Martin
MetroLaser, Inc.,
Irvine, California

J. Seitzman
Georgia Institute of Technology, Atlanta, Georgia

December 1997

FINAL REPORT



ARNOLD ENGINEERING DEVELOPMENT CENTER
ARNOLD AIR FORCE BASE, TENNESSEE
AIR FORCE MATERIAL COMMAND
UNITED STATES AIR FORCE

## NOTICES

When U.S. Government drawings, specifications, or other data are used for any purpose other than a definitely related Government procurement operation, the Government thereby incurs no responsibility nor any obligation whatsoever, and the fact that the Government may have formulated, furnished, or in any way supplied the said drawings, specifications or other data, is not to be regarded by implication or otherwise, or in any manner licensing the holder or any other person or corporation, or conveying any rights or permission to manufacture, use, or sell any patented invention that may in any way be related thereto.

Qualified users may obtain copies of this report from the Defense Technical Information Center.

References to named commercial products in this report are not to be considered in any sense as an endorsement of the product by the United States Air Force or the Government.

## DESTRUCTION NOTICE

For classified documents, follow the procedures in DoD 5220.22-M, Industrial Security manual, Section II-19 or DoD 5200.1-R, Information Security Program Regulation, Chapter IX.

## APPROVAL STATEMENT

This report has been reviewed and approved.

Kevin Zysk
AEDC/DOT
Arnold Engineering Development Center
Arnold AFB, TN

Approved for publication:

FOR THE COMMANDER

# Report Documentation Page

Form Approved
OMB No. 0704-0188



| 1. AGENCY USE ONLY *(Leave blank)* | 2. REPORT DATE | 3. REPORT TYPE AND DATES COVERED |
|---|---|---|
| | 13-Feb-98 | Final Report 05/08/97 – 02/07/98 |

**4. TITLE AND SUBTITLE**

Optical instrument to measure the mass concentration and size distribution of smoke particles

**5. FUNDING NUMBERS**

C: F40600-97-C-0009

**6. AUTHOR(S)**

Stefan R. Martin and Jerry Seitzman

**7. PERFORMING ORGANIZATION NAME(S) AND ADDRESS(ES)**

MetroLaser, Inc.
18010 Skypark Circle #100
Irvine, CA 92614-6428

**8. PERFORMING ORGANIZATION REPORT NO.**

TAR1FINL.DOC

**9. SPONSORING/MONITORING AGENCY NAME(S) AND ADDRESS(ES)**

AEDC/DOT
M/S 9011
1099 Avenue C
Arnold Air Force Base, TN 37389-9011

**10. SPONSORING/MONITORING AGENCY REPORT NUMBER**

**11. SUPPLEMENTARY NOTES**

**12a. DISTRIBUTION/AVAILABILITY STATEMENT**

Approved for public release; distribution is unlimited.

**12b. DISTRIBUTION CODE**

B

**16. Abstract**

This final report describes the experimental work and theoretical modeling done to support the proposed development of a system to measure *in situ* and in real time, the size distribution and mass concentration of soot particles in turbojet exhausts. The proposed system will work in highly turbulent environments. The Phase I work included analysis of laser induced incandescence (LII) signals from soot particles using a numerical model. A breadboard was built to conduct proof of concept experiments, and the main operating parameters and the performance accuracy of a future field system were tested. The availability of a purpose built artificial soot generator enabled quantitative testing of the linearity of the LII signal with concentration and particle size. The results show that an LII system for engine test cells is feasible, and would give accurate measurements of carbon concentration over several decades of soot concentration. Particle size effects have a small influence on the linearity of the LII signal.

**14. SUBJECT TERMS**

Laser induced incandescence, soot volume fraction

**15. NUMBER OF PAGES**

24

**16. PRICE CODE**

| 17. SECURITY CLASSIFICATION OF REPORT | 18. SECURITY CLASSIFICATION OF THIS PAGE | 19. SECURITY CLASSIFICATION OF ABSTRACT | 20. LIMITATION OF ABSTRACT |
|---|---|---|---|
| Unclassified | Unclassified | Unclassified | SAR |

NSN 7540-01-280-5500

Standard Form 298 (Rev. 2-89)
Prescribed by ANSI Std. 239-18
298-102

## PREFACE

The work reported herein was conducted by the Arnold Engineering Development Center (AEDC), Air Force Development Command, at the request of.....

# TABLE OF CONTENTS

# LIST OF FIGURES

## LIST OF TABLES

## INTRODUCTION

This report describes the research undertaken to evaluate the performance of a proposed system to measure *in situ* and in real time, the size distribution and mass concentration of soot particles in turbojet exhausts. The proposed system is based on laser-induced incandescence (LII) and yields signals dependent mainly on soot mass concentration and partially on particle size. The primary objective of the Phase I research was to evaluate the feasibility of implementing the LII technique for the measurement of soot particles in turbulent exhaust flows from turbojet and other engines. Despite much research on Laser Induced Incandescence, mainly in flames, the reliability of the technique for quantitative measurements of soot concentration has not been clearly demonstrated. Therefore, laboratory experiments were conducted during Phase I to test the relationship between the LII signal and the concentration and size of soot particles in a hot gas flow. An essential tool in this work was a laboratory source of simulated soot particles capable of producing precisely known soot concentrations. This device also produced soot particles in certain controllable size ranges, allowing testing of the particle size dependence of the LII signal. Theoretical studies using a computer model of the LII signal backed up the experimental effort.

## TECHNICAL OBJECTIVES OF PHASE I PROGRAM

The following objectives were set out in the Phase I proposal.

1. Model the LII signal as a function of mass, concentration and laser power.
2. Through modeling, decide on a heating source.
3. Define a measurement strategy to isolate the LII signal from potential interfering signals.
4. Experimentally measure the soot concentration, <C>, from 100 $\mu g/m^3$ in a hot turbulent flow.
5. Experimentally demonstrate the linearity of the LII signal over a wide range of concentrations up to 10 $mg/m^3$.
6. Extrapolate the signal to noise ratio (SNR) achieved in the laboratory to conditions at AEDC.

## THEORETICAL BACKGROUND

### Laser-Induced Incandescence

Laser-induced incandescence (LII) occurs when a high power laser beam is absorbed by dispersed particulate matter. This causes the particles to heat up and, at the same time, to lose energy to the surrounding environment by various heat transfer mechanisms: conduction, radiation and vaporization. If the energy absorption rate is sufficiently high, the particle temperature will rise to levels where mass loss through vaporization becomes the dominant cooling mechanism. At these high temperatures, typically a few thousand degrees Kelvin, the particles have significant incandescence and emit radiation in an essentially blackbody spectrum. This radiation is the LII signal and it contains information about the mass concentration and size distribution of the illuminated particles.

Since soot is composed of agglomerates of small particles (called primary particles), each much smaller than the wavelength of visible light, they behave as volume absorbers. Therefore the

overall energy absorption of the primary particles is proportional to their mass (or volume at fixed density) rather than their surface area, which would be the case for larger bodies. If all primary soot particles reached the same temperature, then the LII signal would scale with soot volume or mass; however, the dominant energy loss mechanisms, conductive cooling and vaporization, are proportional to soot size or surface area. Thus the LII signal is not exactly proportional to soot volume ($d^3$). For example, Melton[1] showed using a combination of theory and numerical simulation, that the LII signal scales as $d^m$, with $m=3+0.154\lambda_{det}^{-1}$ and $\lambda_{det}$ is the detection wavelength in micrometers. To produce this result, he ignored conductive and radiative cooling and assumed that the LII signal from a particle is characterized not by its temperature time history but solely by its peak temperature. In essence, this and other analyses[2] indicate that large particles have lower cooling rates and therefore reach higher temperatures compared to small particles. Thus in addition to soot mass, one should also expect LII to be somewhat dependent on particle size and to a lesser extent, other parameters that control cooling rates, for example, gas temperature and pressure.

In outline then, the LII signal is obtained by quickly heating the soot particles with a high power pulsed laser and observing the radiative emission from the hot soot particles. Various models have been developed to account for the heating and cooling mechanisms of the soot particles and for selecting optimum measurement parameters such as collection wavelength, laser power and pulse width, and collection time gates. These models demonstrate the ability to measure soot mass concentration but they also demonstrate the sensitivity of the measurements to the local gas temperature and primary soot particle size. Amongst others, Melton[1], Seitzman[2], and Santoro[3] have developed theoretical and semi-empirical strategies aimed at accurately measuring the soot mass concentration and particle size. Seitzman[2] showed that the local gas temperature and primary soot particle size can have an influence on the LII signal and must be accounted for. Santoro[3] has compared the LII signal to line of sight extinction and scattering measurements. These line of sight measurements require multiple views and tomographic inversion and would be subject to significant errors in turbulent environments caused by beam wandering. Various LII signal reduction strategies have also been considered by these researchers.

Since the LII signal is principally black body radiation, a broad wavelength range is available for measurements; however, wavelength selection must take into account possible fluorescence signals from unburned hydrocarbons in the plume and possible plume luminescence. Also, soot particle size itself affects the emission and absorption of radiation, which means that the wavelength of the incident radiation may also affect the LII signal.

The advantage of LII compared to extinction-based methods is the potential capability of making instantaneous planar measurements of soot volume fraction, rather than measurements averaged along the line of sight or tomographically inverted field measurements. Unlike elastic scattering measurements, LII has a lower potential for significant interference from extraneous factors like the presence of liquid droplets inside the measurement volume. Elastic scattering and interferences from other sources, for example, Raman scattering and laser-induced fluorescence from atoms and molecules (PAH, $C_2$, etc.), can be removed from LII measurements by an appropriate choice of detection wavelength band. Flame luminosity could also interfere but it occurs predominantly at

long wavelengths since it is associated with the much lower temperature of the soot particles outside the laser beam. That limits its effect.

### Light Scattering

Light scattering techniques based on single particle scattering cannot measure the size distribution of submicron soot particles. Single particle counters based on scattered light intensity, polarization, phase, visibility, etc., provide detailed information on particle distribution but are limited to measuring particles larger than about 0.3 μm. In contrast, soot particles are typically extended aggregates of about 20 nm primary particles with an average equivalent diameter smaller than about 0.1 μm. Ensemble measurement devices such as transmissometers and nephelometers do not, in general, provide detailed information of the size distribution and significant assumptions have to be made to correlate measured bulk averages to detailed distribution information. Nevertheless, since soot may be regarded as a fractal aggregate of near single size particles, these ensemble light scattering techniques have provided useful information; however, these techniques are sufficiently complex in implementation to be impractical for applications in the difficult environment of an engine test cell.

## EXPERIMENTAL SETUP

The aims of the experimental program were to produce well known volume concentrations of soot particles and use them to test the linearity of the LII signal with concentration. The incorporation of a heating element allowed the influence of the surrounding gas temperature on the LII signal to be tested. Also, particle size dependencies could be measured. Scattered light measurements were also made to test the possibility of establishing a mean particle diameter from the polarization of the scattered light.

### LII system

The LII system was set up in two ways. An initial set of experiments was performed using a monochromator which allowed a very narrow wavelength selection. Later sets of data were taken with a simplified optical system which gave much higher optical sensitivity. Also, the detection and signal processing arrangements were improved. The first setup allowed a baseline set of measurements to be taken from which an extended and enhanced measurement program could proceed.

*Setup 1:*

This setup employed a Nd:YAG laser producing 180 mJ, 7 ns (full-width half maximum) pulses at 10 Hz (see Figure 2 for an example laser pulse). The 532 nm laser beam was focused and apertured to form an almost uniform laser sheet approximately 7 mm high and 200 μm wide. The detection system consisted of a set of slits defining a measurement area of 1.5 x 2.5 mm, a monochromator and a photomultiplier tube. To increase the sensitivity of the system, the monochromator slits were opened to a width of 2.9 mm, giving a bandwidth of about 6 nm. LII measurements were made at a center wavelength of 650 nm.

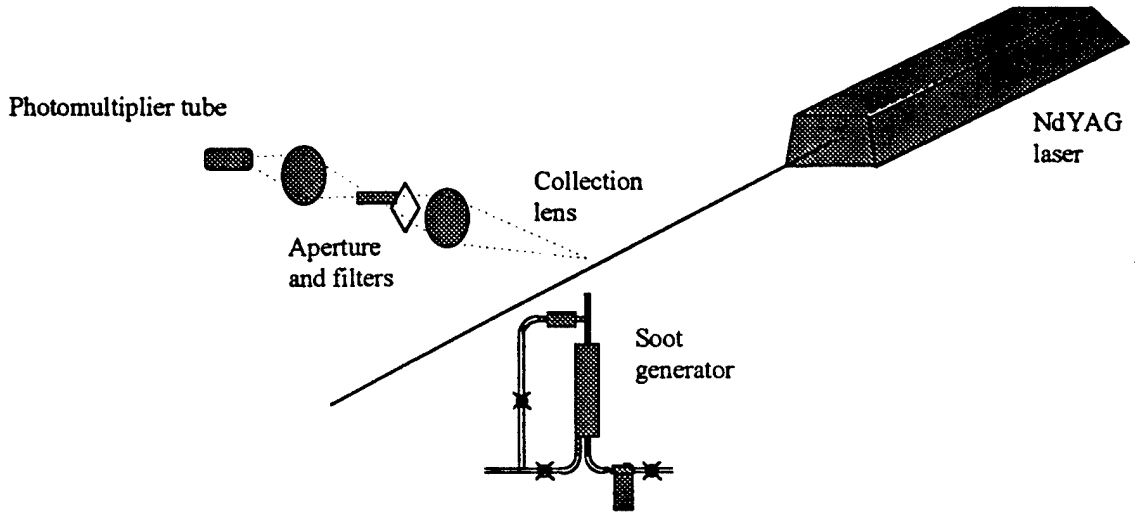


**Figure 1. Layout of LII system, setup 2.**

LII signals were fed into a boxcar circuit which averaged 100 pulses and then a set of different measurements were made on the resulting signal. These measurements were the peak signal and the mean signals over 30 ns and 90 ns time intervals starting just before the laser pulse. In an optimized system it is expected that the necessary averaging times would be much shorter than the ten seconds or so required here.

A further set of measurements was made using different measurement criteria. These were: LII signal integration over 500 ns using the oscilloscope, LII signal integration over 500 ns using the boxcar, and LII signal amplitude measurements at the peak, and 50 ns and 250 ns after the pulse.

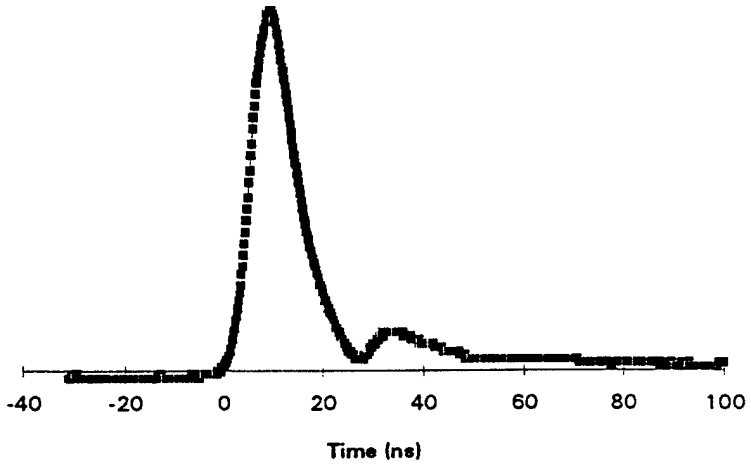


**Figure 2: The laser pulse. The small second peak is a measurement artifact due to electronic ringing; it is not present in the optical signal.**

*Setup 2:*

In this second optical setup (see Figure 1), the system was simplified and optimized to produce a high efficiency detection system, allowing the sensitivity range to be greatly extended.

For this second set of experiments we used the fundamental mode (1064 nm and 250 mJ pulses) of the Nd:YAG laser. This was to eliminate the possibility of detecting elastically scattered light; the photomultiplier sensitivity extended only to a little beyond 800 nm. Also, it would reduce any possible dependence of absorption cross-section on agglomerate particle size and minimize interferences associated with emissions from laser-produced $C_2$ molecules. The laser beam was unfocused and formed a cylindrical volume about 8 mm in diameter. The detection system was modified so that it viewed a region within the laser beam approximately 3 mm high by 8 mm wide. The monochromator previously used was dispensed with and colored glass filters were used to set the wavelength band to 570 to 800 nm. The sensitivity of the photomultiplier tube (PMT) photocathode itself formed the long wavelength cut-off. The PMT was operated at constant voltage and neutral density filters were inserted as necessary to maintain the photocurrent within acceptable limits.

LII signals were fed directly to a Tektronix digital oscilloscope which averaged 128 pulses. For immediate return of data a mean was taken over the first 50 ns of the signal, and for later analysis, the complete LII decay signals were transferred to a PC. Scattering measurements were made using the same method, but since the signal is static, no recording was done.

For the LII measurements, we took a simple integration over 50 ns and employed only the oscilloscope as a data collection and processing device. This, combined with our improved optical system, produced superior data and reduced measurement uncertainty.

**The soot generator**

The soot generator consists of two main components, a nebulizer and a dryer. The nebulizer is connected to an air supply and produces a fine mist of small particles from a fluid placed in its base. When using pure water, the particles have a mean diameter between about 3 and 8 μm, depending on the air flow and on the nebulizer itself. To produce soot particles, we dispersed carbon black in water and placed this in the nebulizer. Thus, small droplets of water were produced by the nebulizer which contained a certain amount of carbon. This water was evaporated inside the dryer, which consists simply of a heated cylinder open at one end.

The soot generator was set up in a vertical orientation, as shown in Figure 3. Two air supplies were connected to the system, one to the nebulizer and the other to a bypass air supply which was used to dilute the output of the nebulizer. The drying unit was heated to ~100° C, resulting in an output air temperature of about 70° C. Soot volume fraction was varied in two ways: one, by increasing the amount of dilution air supplied to the bypass system, and two, by varying the concentration of the carbon/water mix in the nebulizer. Throughout the experimental procedures the nebulizer was run at a constant air flow rate of 9.24 l/min. Each air supply line was regulated using a valve, pressure gauge and flow meter so that exact volume fractions of soot to air could

be calculated. The output of the soot generator was a tube forming a uniform flow of material about 14 mm in diameter. Measurements were made within approximately 15 mm of the end of the tube. Table 1 summarizes the operating parameters for the soot generator and laser systems used under setup 2.

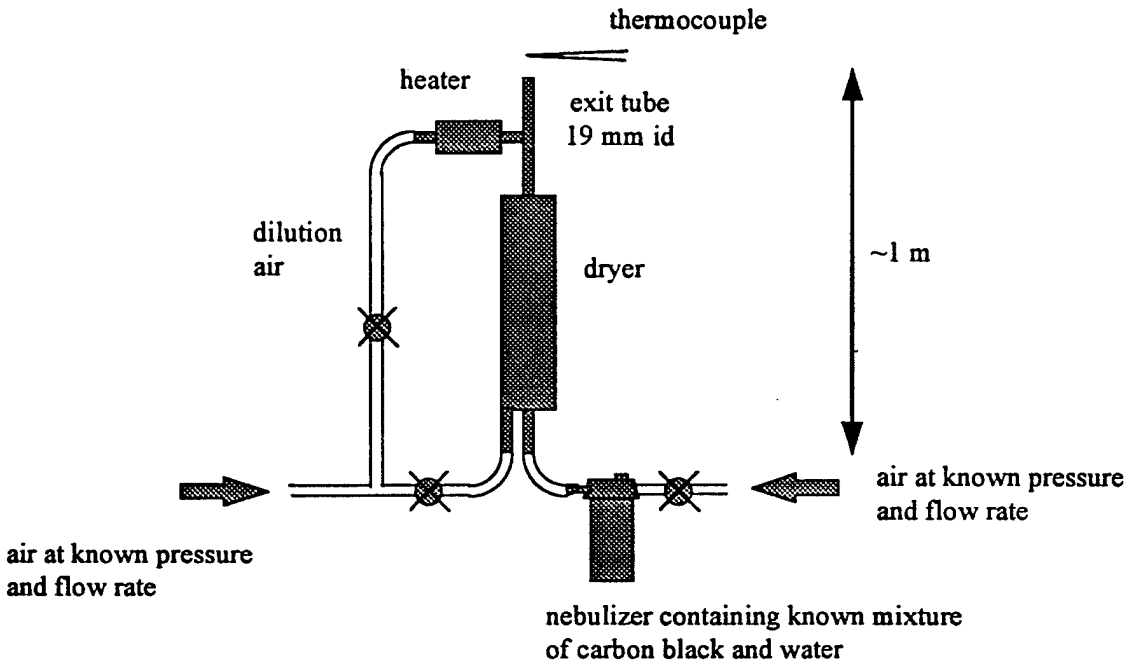


**Figure 3: Layout of nebulizer and dryer.**

The carbon black material, Cabot 800, is composed of 17 nm primary particles. Insoluble in pure water, it was weighed out using an electronic balance and dispersed in distilled water using Winsor and Newton gum arabic so that each half liter of water contained 2.8 g of carbon black, and 0.5 ml of gum. This mixture was agitated in a blender for at least twenty minutes before use. Further dilutions were then made immediately by adding distilled water alone to portions of the original mixture.

**Table 1: Settings for the experimental measurements using Setup 2.**

| | | | |
|---|---|---|---|
| Nebulizer production rate | 0.337 ml/min | 34 psi | 10 scfm |
| Carbon production rate (maximum) | 18.9 mg/min | | |
| Dryer temperatures | 100° C wall | 70° C outlet | |
| Nd:YAG pulse | 250 mJ /pulse | 7 ns | 500 mJ/cm$^2$ |
| Argon laser | 65 mW | | |
| LII filters | OG 550, OG 570 | > 570 nm | |
| Collection aperture | f/4.5 | | |
| Measurement volume | 0.2 cm$^3$ | | |
| Number of samples | 128 | | |

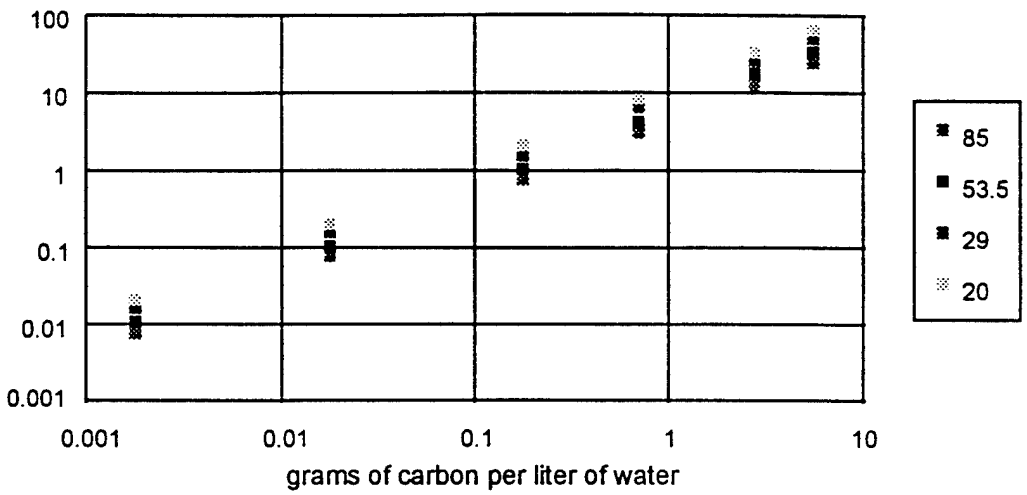


**Figure 4: Carbon concentration produced by varying the concentration of carbon in the nebulizer and by varying the dilution air setting. The legend shows the air flow setting in arbitrary units.**

By varying the concentration of the fluid in the nebulizer, a greater range of soot volume fraction could be obtained. This actually produces two effects: one, dilution of the fluid reduces the concentration of carbon in the droplets that the nebulizer produces, resulting in a lower volume fraction of carbon in the drier outlet, and two, it reduces the size of the agglomerated soot particle (as will be discussed below). Figure 4 shows graphically the range of carbon concentrations employed in the experimental work. Various air settings (labeled 85, 53.5, etc.) varied the carbon concentration over small ranges (a factor of 2 or so), and a large overall range was gained by varying the amount of carbon in the water. At the lowest concentration the water appeared almost clear, whilst at the highest, it had the appearance of ink.

*Particle dynamics and morphology*

The carbon particles produced by the soot generator, while similar to soot particles, have a different morphology. To explain why, we consider the forces that very small particles experience. First, electrostatic forces are very large. The attractive force between two 30 nm diameter particles of opposite charge of one electron is 0.25 $10^{-12}$ N. The mass of a 30 nm diameter soot particle is about $3\times10^{-20}$ kg, so the acceleration when they are very close together is about $10^{6}$ m/s. Surface tension forces are even larger; for two 30 nm particles enclosed by a liquid the force holding them together is about $2\times10^{-9}$ N. Electron micrographs of soot particles are available in the literature: these show extended objects composed of many small particles (see Figure 5). These come together through collisions and electrostatic forces and stay together despite the turbulence of the combustion process because of the strength of electrostatic and surface tension forces between them.

The particles generated by the soot generator are different to those normally produced in a flame. The primary carbon black particles which are produced by burning fuel are about 17 nm in diameter. When the nebulizer produces a droplet of water, that droplet contains a large number of

primary particles (see the estimates in Table 2, based on an initial 8 μm droplet size). Evaporation of the water in the dryer then reduces the diameter of the water droplet, which retains its spherical shape. Surface tension forces crush the soot particles together to form a spherical ball of carbon, rather than the typical extended object produced in a sooting flame.

Small soot particle generated in a flame

Small soot generator particle with gum arabic

**Figure 5: Soot particle morphology.**

Furthermore, we needed to add gum arabic to disperse the carbon into the water. Tests showed that this material produced no LII signal itself but it could conceivably influence the LII signal of a carbon particle by affecting the vaporization rate or temperature by, for example, boiling at a low temperature during the laser pulse. A residual amount of this gum will be included in the particle aggregate as interstitial material. Tests on the evaporation of gum show that the amount of gum left in each soot particle after drying would be about 6% by weight. If the residence time of the particle in the dryer was short though, some of the evaporable component of the gum (mainly water) might not dry off, so the particle could produce a different LII signal. This signal should be less because the water in the gum will act as a heat sink while the particle is subjected to the laser pulse. Therefore, the measured LII signals might be expected to have some dependence on air dilution flow rates, and even for a given liquid dilution, the LII signals may not scale exactly with soot concentration because of different drying times.

**Table 2: Estimated sizes and masses of soot particles produced by the soot generator.**

| Fluid dilution <C> (g/l) | Diameter of carbon (nm) | Diameter of gum droplet (nm) | Carbon particle mass (kg) | Number of primary particles |
|---|---|---|---|---|
| 5.6 | 956 | 409 | 1.6 * 10-17 | 286000 |
| 2.8 | 759 | 324 | 7.9 * 10-18 | 14300 |
| 0.0175 | 140 | 60 | 4.9 * 10-20 | 896 |
| 0.00175 | 65 | 28 | 4.9 * 10-21 | 90 |

We therefore expect that the soot generator presents a worst case test of the linearity of the LII technique. Combustion produces soot particles that are extended aggregates which can be expected to give signals representative of individual small particles of carbon. In contrast, the soot

generator produces particles that are more or less solid spheres, giving LII signals which are expected to have a particle size dependence. Also, the soot generator enables the influence of extraneous materials present in the soot, in this case gum, to be ascertained.

### Light scattering

An Argon ion laser was set up to enable scattering measurements on the soot particles. Scattering measurements were made at 514.5 nm. The laser beam was vertically polarized. A Polaroid filter mounted in a rotatable mount was used to enable detection in two orthogonal polarization directions. The viewed volume was somewhat smaller than that seen by the LII system, only about 1.2 mm diameter and 7 mm long. A high sensitivity photomultiplier tube was coupled through an optical fiber to form the detection system. The optical system is illustrated in Figure 6. Scattering measurements were made using the oscilloscope's calculation facilities and taking an average over about 20 seconds. These relatively long averaging times were adopted because of instability of the Argon ion laser output power.

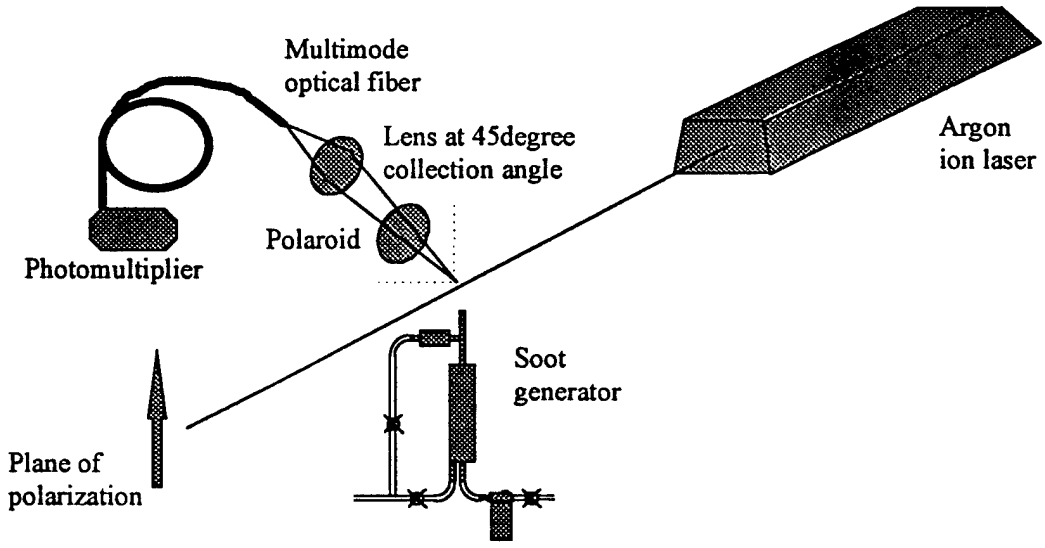


**Figure 6: Layout of light scattering system.**

## EXPERIMENTAL MEASUREMENTS

To obtain the wide range of 3 orders of volume fraction, both the dilution air flow rate and the concentration of the fluid in the nebulizer were varied. As the concentration of carbon in the fluid is varied, this results in a change in the size of the agglomerated soot particle.

### LII signal amplitude

*Tests using optical setup 1*

Initial tests were made using distilled water and gum arabic and no carbon black. When nebulized and passed through the drier, the mixture produced negligible scattering and LII signals. A series of measurements were then made using the 'standard' mixture of 5.6 g <C>/l. By varying the

dilution air flow the concentration of carbon in the outlet could be varied. One hundred LII signals were averaged in the boxcar and then the peak signal and the mean signals over 30 ns and 90 ns time intervals were measured. Calculations of the volume fraction of carbon in the dryer outlet were made from the air flow rate and pressure gauges, and from the rate of loss of fluid from the nebulizer which was measured several times over about one hour.

Measurements made with this setup did not differ significantly from those made later with the improved optical system, so to avoid repetition they will not be described here.

We made a further set of measurements using a range of different measurement criteria. These were: LII signal integration over 500 ns using the oscilloscope, LII signal integration over 500 ns using the boxcar, and LII signal amplitude measurements at the peak, and 50 ns and 250 ns after the pulse. This resulted in a set of data made at a constant air dilution, and only varying the concentration and particle size. The results are shown in Figure 7. Here the boxcar and oscilloscope integrations and the signal amplitude at 50 ns scale well with concentration and independently of particle size, whilst other measurement strategies such as the peak (13 ns), scattered light and long integration (250 ns) give very non-linear results.

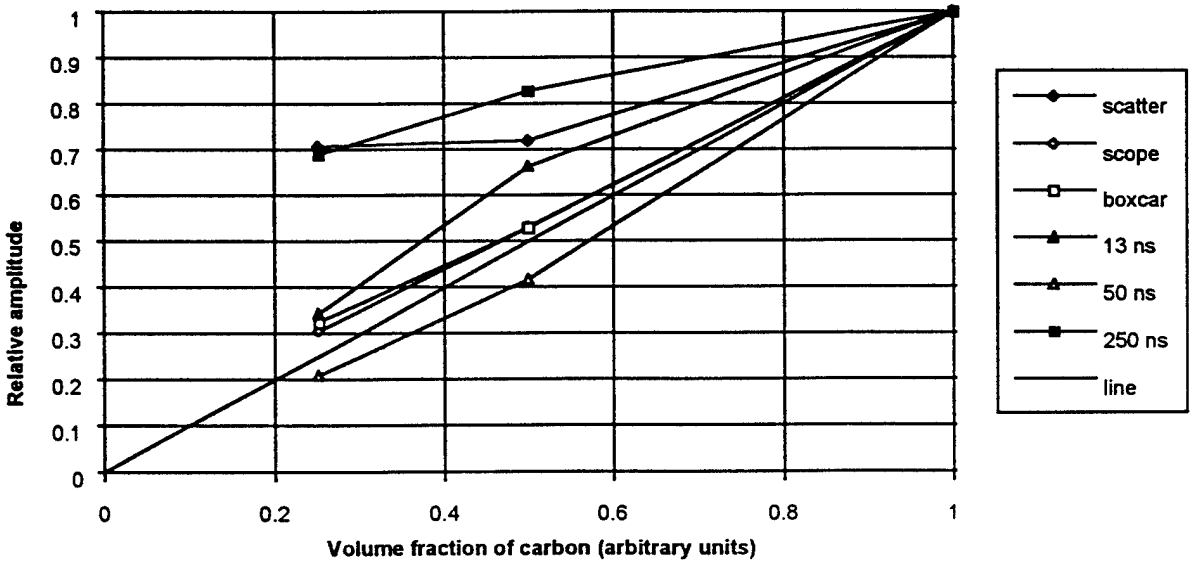


**Figure 7: LII and scattering signal amplitudes as a function of carbon concentration, taken by various measurement methods. Four different dilutions of carbon suspension were used.**

These results show that the measurement method adopted has a large effect on the signal linearity and that closer agreement with carbon volume fraction can be obtained by adopting the right measurement methods. There is clear evidence of a particle size effect, not surprising in the scattered light measurements, but also not unexpected in the LII measurements. This brings the hope that after appropriate model development, we might use it to determine soot particle sizes.

## Tests using optical setup 2

In the second and main set of experiments the infra-red, 1064 nm output of the laser was used and the optical system was simplified and optimized to produce a high efficiency detection system, allowing the sensitivity range to be greatly extended.

The simplified optical system described on page 5 was used for these measurements. We dispensed with the boxcar and fed LII signals directly to a Tektronix digital oscilloscope which averaged 128 pulses. For immediate return of data a gated mean was taken over the first 50 ns of the signal and read directly off the oscilloscope, and for later analysis, the complete LII decay signals were downloaded to a PC. New scattering measurements were made using the same method, but since the signal is static, no recording was done.

To obtain a wide range of more than 3 orders of magnitude of volume fraction, both the dilution air and the concentration of the fluid in the nebulizer were varied. As the concentration of carbon in the fluid is reduced, the size of the agglomerated soot particle changes since less carbon material is contained in each water droplet. The mean soot particle size is therefore proportional to the cube root of the carbon concentration. Table 1 shows typical soot particle characteristics.

In the measurements made using Setup 1, it was found that different measurement approaches resulted in different signal/concentration responses. This time we used a simple integration over 50 ns and used only the oscilloscope as a data collection and processing device. This, combined with our improved optical system, gave better data with reduced measurement uncertainty. In the previous measurements, a 50 ns measurement gave an almost linear response.

*LII measurements over a wide concentration range*

Initial conditions were established using distilled water to obtain a satisfactorily low background. Photomultiplier sensitivity was adjusted by placing neutral density filters in the optical path rather than by changing the gain of the tube. This had the benefit of maintaining constant electronic delays within the PMT, and thus no adjustment of the acquisition gates was required. With each dilution, the concentration of carbon was further varied by altering the dilution air flow.

LII signal measurements were made by taking the mean signal over a 50 ns gate, and averaging 128 signals. Referring to Figure 8, there are six sets of data. Each set of data is made at a certain nebulizer fluid concentration, and only the dilution air flow is varied. Hence, the mean soot particle size is different for each set. Therefore this graph shows two effects: one, the change in LII signal with concentration of carbon alone, and two, the change in LII signal with concentration and soot particle size.

The overall slope of logarithm of the LII signal amplitude with the logarithm of concentration is ~1.07. The LII signal therefore appears to be nearly proportional to volume fraction of soot for fixed particle size distribution. Within each data subset, there is a degree of scatter that results in calculated slopes that are not statistically distinguishable from the overall data.

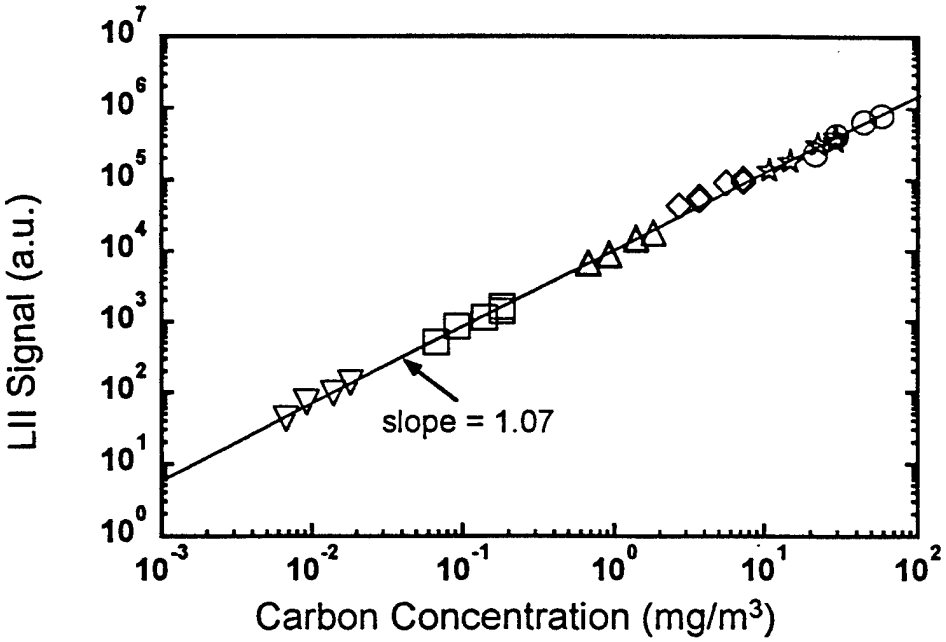


**Figure 8: LII signal as a function of carbon concentration.**

The ultimate detection limit in our experimental setup is at least one order of magnitude lower than reported here. At the lowest carbon concentration we still had one ND 1 filter (which attenuates the signal by an order of magnitude) in our optical system. Since we measured a carbon concentration as low as 8 $\mu g/m^3$ in a volume of approximately 0.2 $cm^3$, these results show that we could measure a concentration as low as 0.8 $\mu g/m^3$ under the same conditions simply by removing the filter. Therefore a quantity of 0.16 $10^{-12}$ g of C can be measured using 128 laser shots, or at worst a quantity of 21 $10^{-12}$ g of C can be measured with 1 shot.

**Measurement strategies**

The above LII signal measurements were made by taking the mean signal over a 50 ns gate, and averaging 128 signals. Again, this resulted in proportionality of the LII signal amplitude with the concentration of carbon raised to the power 1.07, which we interpreted as a particle size dependence of the LII signal. We can convert the concentration dependence to size dependence by recognizing that the diameter of a soot particle produced from a fixed size water droplet scales with the cube root of the soot concentration in the droplet. Thus, our results suggest a size dependence of $\sim d^{3.21}$.

This is in reasonable agreement with Melton's[1] simplified analysis, which assumes a temperature constant in time but dependent on particle size: effectively therefore the LII signal would be measured during the laser pulse. This results in the approximate dependence: LII $\propto d^{3+0.154/\lambda}$, or $d^{3.19}$ to $d^{3.26}$ for our detection range of ~600-800 nm. Since vaporization of the particles is taking place, there will also be a small but continuous change in particle size and temperature. The size dependence is primarily a result of larger particles getting hotter than smaller particles, thus increasing their relative contribution to the LII signal. This applies when all the particles are within the Rayleigh range where energy absorption is volumetric and cooling scales more closely

to particle surface area. McManus *et al*[4] suggested that a measurement of the signal would be better made after the particles cool to the vaporization temperature. This is because they will cool rapidly to the vaporization temperature and then more slowly, primarily by conduction. At this moment the dispersion of temperatures is therefore at a minimum, and the LII signal may be more nearly proportional to soot concentration.

The previously stored LII signals were analyzed for signal strength 26 ns after the beginning of the laser pulse, i.e., just at the end of the pulse. The results are shown in Figure 9. There was a little electronic ringing visible on the signal which reduced the accuracy of these measurements, but they yielded a power dependence on concentration of 1.09, close to the 1.07 value for the prompt LII signal. The standard error in the measured slope of Figure 9 is about 0.03, so these measurements are not significantly different.

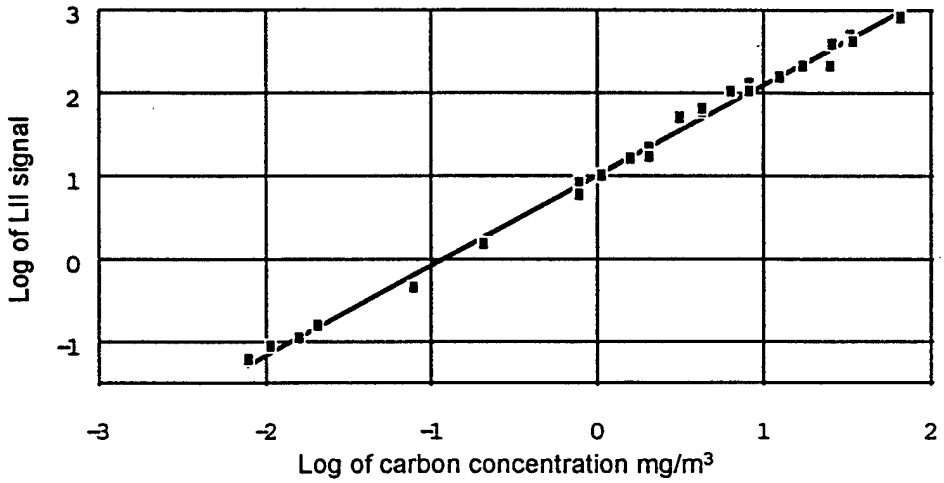


**Figure 9: LII signal dependence on soot concentration for a 5 ns gate starting 26 ns after the beginning of the laser pulse, showing the best fit line with a slope of 1.09.**

We then plotted relative LII signal divided by carbon concentration against soot particle size and obtained the graph shown in Figure 10. In other words, we assumed the variation in calibration constant was entirely due to particle size variation and that the LII signal is otherwise proportional to soot concentration. The graph shows a smooth variation of the LII calibration constant as the soot particle size changes. The graph shows a peak to peak variation of 2.5 for the calibration factor between the LII signal and the carbon concentration. Note that in an engine, it is expected that the particle size would be held within a much smaller range and also that the soot particles would be extended objects rather than spheres. These two factors would yield a much tighter correlation between LII signal and carbon concentration.

Data at the right end of each group in Figure 8 are for the highest concentration of carbon and therefore the lowest dilution air flows. The residence time for particles in the dryer was a maximum, and the drying most efficient. Therefore the LII signal should be greater than for particles at the lowest concentration, however the scatter in the individual data sets is too large to see an obvious effect.

We can conclude that the system studied represents a worst case. In general, soot particles are extended aggregates and can be expected to give signals representative of individual small particles of carbon. It also is encouraging in that the influence of extraneous material, in this case gum, and in the real case unburned fuel and PAH, appears to have little effect on the LII signal.

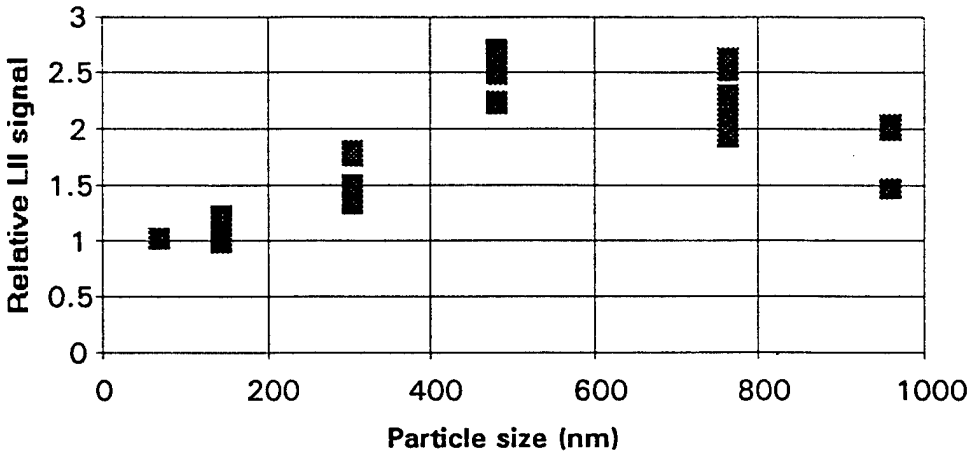


**Figure 10: The LII signal as a function of soot particle size assuming a linear dependence on soot concentration and that the nebulizer produces 8 μm water droplets.**

*Particle size effects*

Figure 10 on page 14 shows the variation of calibration factor with particle size, assuming all the variation is due to particle size. This correspondence was modeled (see Figure 21 on page 22), and produced a graph with a remarkably similar form. (On this plot, we assumed that the mean droplet size produced by the nebulizer was 4 μm, rather than 8 μm. The size of 4 μm was chosen because it corresponded with electron micrograph evidence from a previous set of data for this nebulizer[5]. The 8 μm size was measured on a different but similar nebulizer using light scattering techniques.) The model assumed that the soot particles were solid carbon spheres rather than aggregates so complete correspondence would not be expected, but the results show that the model developed can reproduce features observed in experiments. It does, however, overestimate the error caused by particle size and the diameter scaling is incorrect, which shows that the aggregates we used had slightly different (and better) properties. This encourages us to think that when measuring real soot particles, the error in the calibration constant for extended aggregates will depend only on the small spread in primary particle size and could be as small as 15 or 20% or even less.

**LII signal temporal decay**

Further analysis of the signals concerned measurement of the decay time of the traces.

*Measurements of LII signal decay time.*

The complete LII signals, which contained a mean of 128 traces, were fitted to an exponential decay over the period from 13 ns to 190 ns after the laser pulse. Figure 11 shows a typical signal. Note the rapid initial decay from the peak, signifying vaporization cooling, then the more gradual

curve as conduction cooling takes place. This was the part of the curve which was fitted. Time decay constants $k$ were calculated where the signal $S = S_0 e^{-kt}$. The exponential fit is sensitive to baseline offset and also to noise, and there is a spread of data produced as shown in Figure 12 which plots decay time against particle size. Remarkably, there is no obvious trend in decay time with particle size; in addition to noise and experimental errors, this may result from the large particles produced by the soot generator. Large particles decay slowly (> 1 μs) and it is difficult to measure their decay rate accurately over only 190 ns.

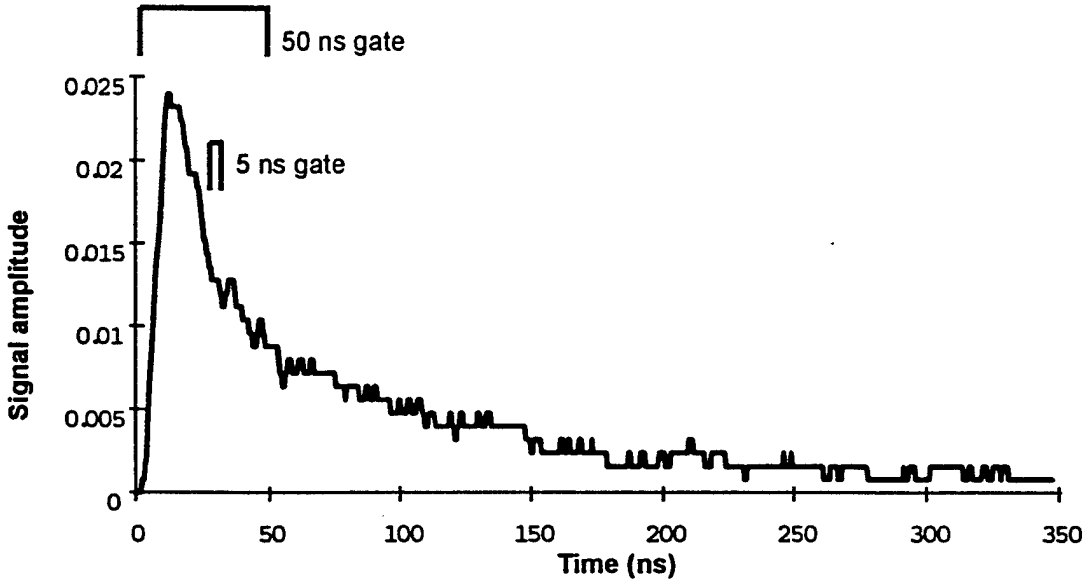


**Figure 11: A typical LII signal showing the position of two of the signal gates used.**

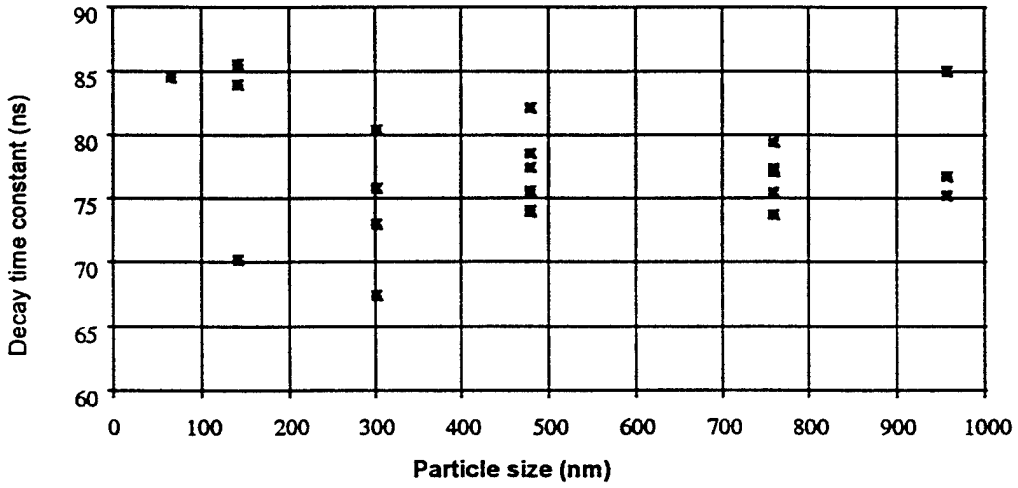


**Figure 12: LII signal time decay constants in nanoseconds as a function of soot particle size.**

## Thermal effects

*LII measurements over a temperature range*

An addition was made to the equipment which allowed a portion of the dilution air to be heated. This hot air was introduced near the top of the dryer, directly into the outlet pipe. This allowed the output gas stream to be heated up to nearly 300°C so that comparisons of the LII signal could be made at different temperatures. It is expected that the LII signal will be slightly larger at a higher temperature since it cools less rapidly; however, the temperature of the gas is still very much lower than that of the incandescent particle, so it should be a small effect. In the experiment, heating the gas reduces its density which in turn decreases the LII signal because the flow velocity through the pipe is higher. The concentration data were corrected for this effect. It can be seen from Figure 13 that the high temperature 330° C (triangles) data lies on the same curve as the data taken at 70° C (boxes). Therefore, at the temperatures tested here, there is little change in the LII signal due to temperature changes in a measurement region.

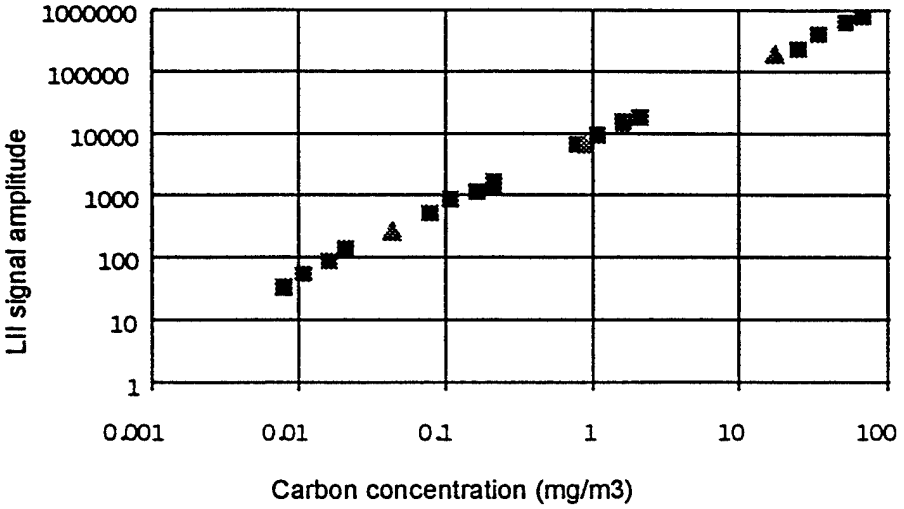


**Figure 13: Dependence of the LII signal on temperature. The boxes are data taken at 70° C, and the triangles data taken at 330° C.**

## Light scattering

*Polarization measurements*

For small particles, the polarization ratio of the elastically scattered light is very high, but for very large particles it approaches unity. Therefore a polarization measurement will give an indication of agglomerate particle size, assuming that the particle is roughly spherical. This particle size measurement could be useful when comparing the LII measurements against gas temperature effects, because agglomerate particle shape and surface area will affect the cooling rate. In addition, a particle size estimate can be used to cross calibrate the LII signal.

Mie scattering calculations were made for spheres under polarized light and using polarized detection. These show that the signal power varies with the sixth power of the diameter for

particles less than 200 μm in diameter (see Figure 14). Also, the scattered light polarization ratio varies with particle size so the ratio of the intensity of the scattered light at two orthogonal polarizations was measured. Figure 15 shows the results and the polarization ratio calculated using Lorenz-Mie scattering theory for small particles between 10 and 1000 nm in diameter (solid line).

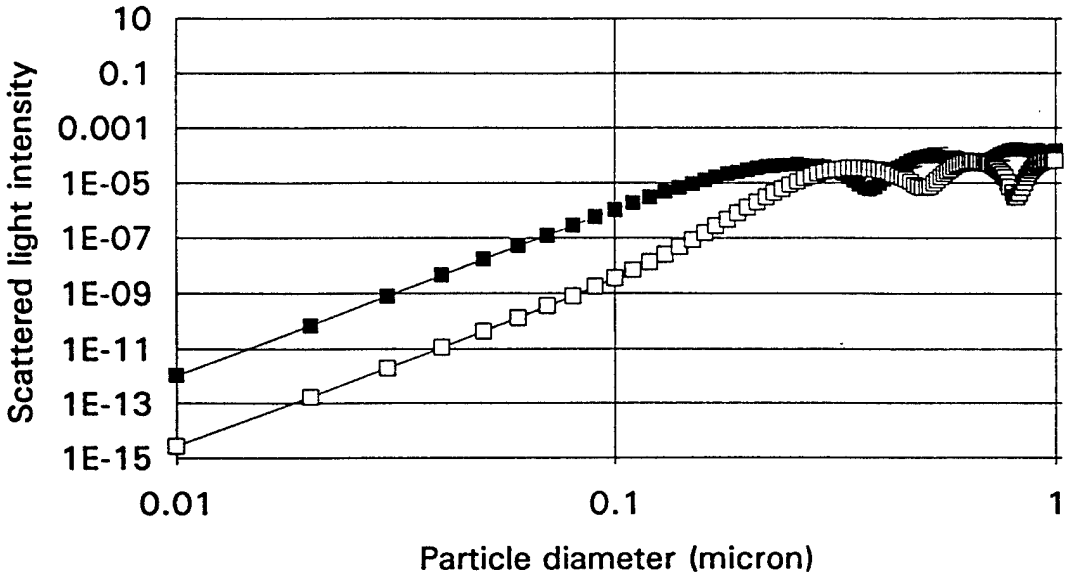


**Figure 14: Theoretical scattered light intensity for in plane (lower curve) and out of plane polarizations (upper curve) for the scattered light detection system. These curves show the scattered light intensity decreasing with the sixth power of the diameter for particle sizes below 200 nm.**

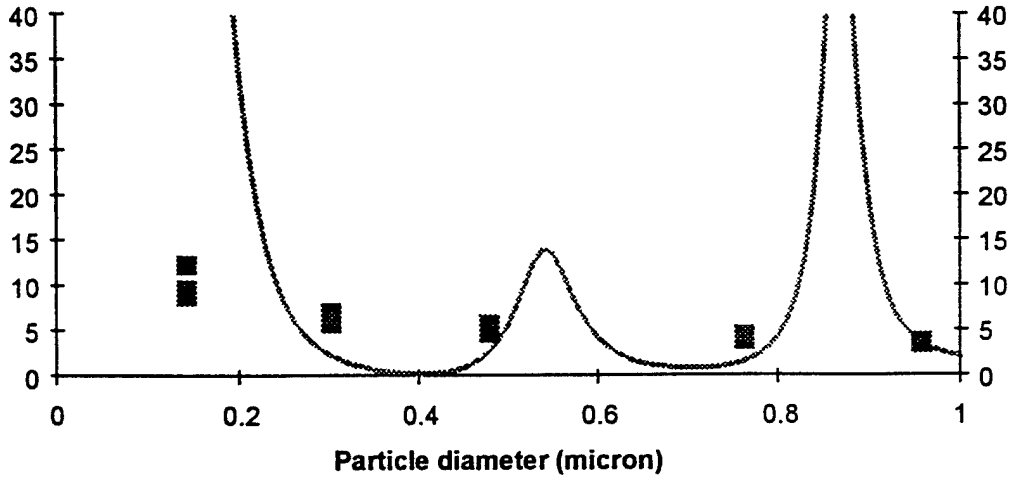


**Figure 15: Theoretical polarization for single spherical particles (line) compared with measured polarization ratio for estimated mean soot particle size (boxes) produced by the soot generator.**

At high polarization ratios, the signal is difficult to measure because the scattered light is weak, and the disturbing effects of stray light in the laboratory and small temperature fluctuations in the detector amplifier circuits contribute to uncertainty in the baseline. Therefore, at the lowest concentration, and smallest particle size, no polarization measurement was attempted. The particle size was estimated from data on the size distribution of water droplets produced by the nebulizer. Clearly there is some discrepancy between the measured polarization ratio and the calculated ratio for the nominal mean diameter. This may be because for very small particles the scattered light intensity falls as the 6th power of particle diameter so that small particles contribute only very little to the overall scattered light. This results in a bias towards the larger particles in the sample. Conversely however, the intensity does not increase smoothly with size (Figure 14) and has local maxima for the two polarizations at about 250 nm and 380 nm, so that the polarization ratio is biased to fall within a certain range.

## MODELING RESULTS

### Laser Induced Incandescence Model

The computer model of the LII process runs under Matlab. It calculates time-dependent size, temperature and incandescence from a primary soot particle exposed to an arbitrary laser pulse. The single particle results are converted to results for agglomerated soot particles by neglecting primary particle interactions. The model is based on standard equations representing the processes of particle heating and cooling[2]. Potential drawbacks of the model include uncertainties in a number of material constants such as specific heat capacity and refractive index. Also there are some effects neglected in the model, for example surface ablation and non-uniform heating for large particles larger than a few hundred nanometers, a size not normally found. Also, the conduction cooling model is problematic for the range between continuum and free molecular flow, and the vaporization model assumes all lost material is vaporized as $C_2$.

The results of the modeling effort lead to certain choices in the experimental setup and also can be used to interpret the experimental results. In these results, an important parameter is C, effectively an LII calibration "constant." It represents the LII signal normalized by the soot concentration; if the LII signal depended only on soot concentration in a linear fashion, that is, signal = C × concentration, then C would be a true constant. Variations in C represent potential systematic errors in the measurement. In the discussion below, we concentrate primarily on the effects of particle size.

### Detection and laser excitation

Figure 16 shows the results of a calculation of C as a function of detection wavelength and particle size. Comparing red and blue detection, one sees that red detection results in less dependence on particle size; both curves have the same slope, but since the red curve is above the blue, the fractional variation in C is less. This is because the incandescent emission intensity at blue wavelengths is more sensitive to particle temperature. Additionally, the higher value of C for red detection indicates a larger signal and therefore red detection can lead to improved signal to noise ratio and increased sensitivity. Restricting detection to the near infrared eliminates the

background signal from hot bodies including nascent soot particles in the rest of the exhaust plume. Plume radiation is weaker than the soot radiation because the gas temperature is very much less than the vaporization temperature of the laser-heated soot.

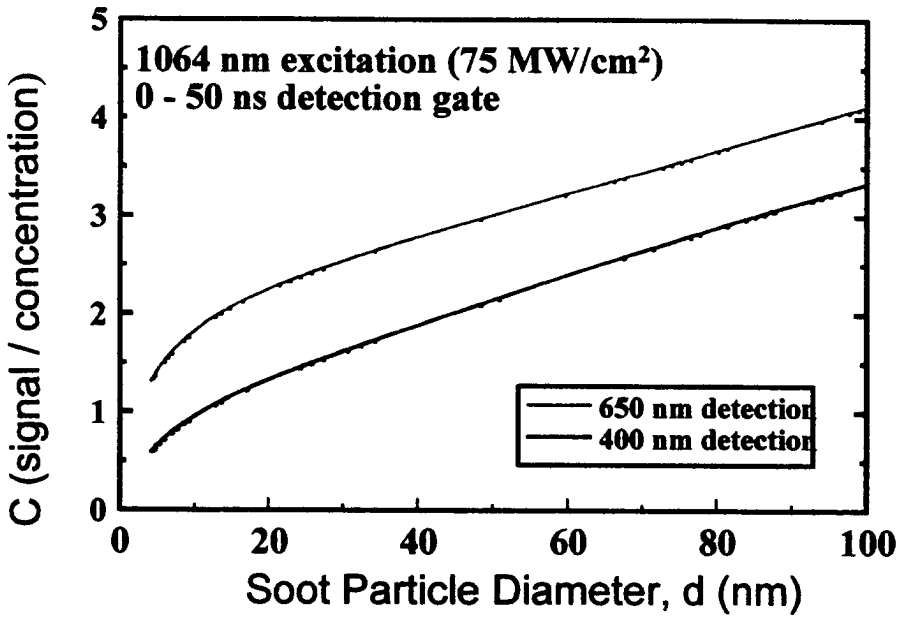


**Figure 16: The calculated variation of the LII calibration factor C with soot primary particle diameter.**

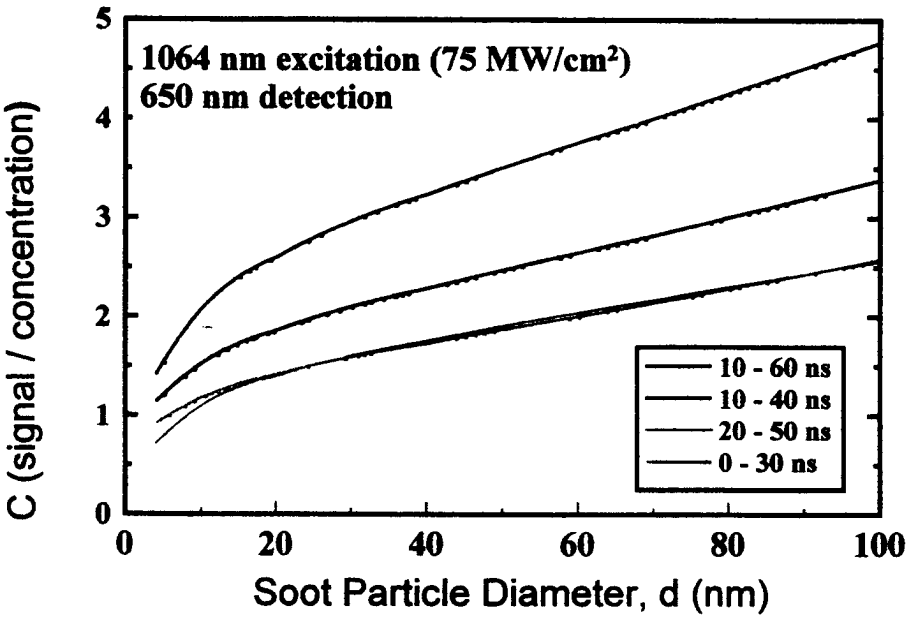


**Figure 17: The calculated variation of the LII calibration factor with soot primary particle diameter and time of the signal gate after the onset of the laser pulse.**

The dependence on particle size can also be reduced by proper choice of temporal detection gating. Figure 17 shows that detecting the signal at times near the peak of the laser pulse minimizes the size dependence, especially for small particles. The size dependence is also reduced if the laser intensity is above the threshold fluence required to heat the smallest particles to the vaporization point. This is seen in Figure 18, where the threshold fluence for infrared (1064 nm) excitation is seen to be 60-80 MW/cm$^2$, or ~0.5 J/cm$^2$ for a 7 ns laser. The use of a long wavelength laser source also ensures that even the larger particles undergo volumetric heating, since it extends the Rayleigh range to larger particle sizes compared to visible wavelength lasers. This may be an advantage in reducing size effects for larger soot agglomerates, when large numbers of primary particles in very close proximity might interact with the heating radiation in a way similar to large single particles.

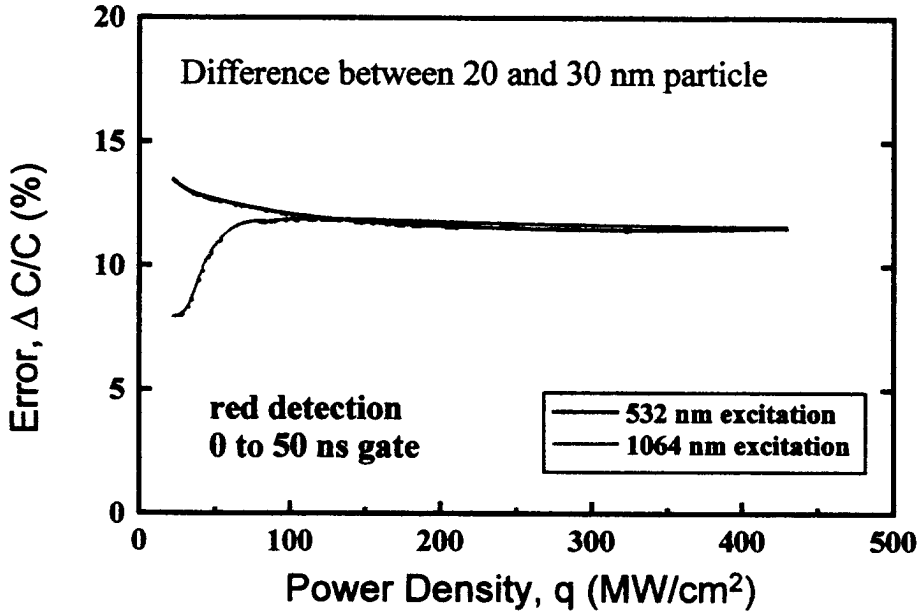


**Figure 18: The calculated change in the LII calibration factor between two particle sizes as a function of laser fluence.**

When particle size effects are considered, we see that the combination of long wavelength excitation and shorter wavelength detection provides a number of advantages. In fact, this strategy also results in reduced scattering interferences for most conditions. Since scattering from small particles scales with $(d/\lambda)^6$, use of an infrared laser reduces the scattering signal from particles by a factor of 64 compared to a green laser source. Scattering from particles and surfaces is also easily filtered without sacrificing incandescent light. For example, scattered infra-red radiation can easily be rejected from the LII signal by the use of a detector which is blind to the infra-red. Laser-produced $C_2$ emission is also greatly reduced for 1064 nm excitation (earlier work by Seitzman shown in Figure 19). What little $C_2$ emission does occur can be avoided by detection at wavelengths longer than about 600 nm or shorter than about 430 nm. For these reasons, we chose to heat the soot using the fundamental wavelength of the Nd:YAG laser (1064 nm) and detect the LII signal between wavelengths of 600 nm and 800 nm using a PMT. The

short wavelength cut-off was selected by a colored glass filter, and the PMT photocathode, insensitive to wavelengths greater than 800 nm, formed the long wavelength cut-off.

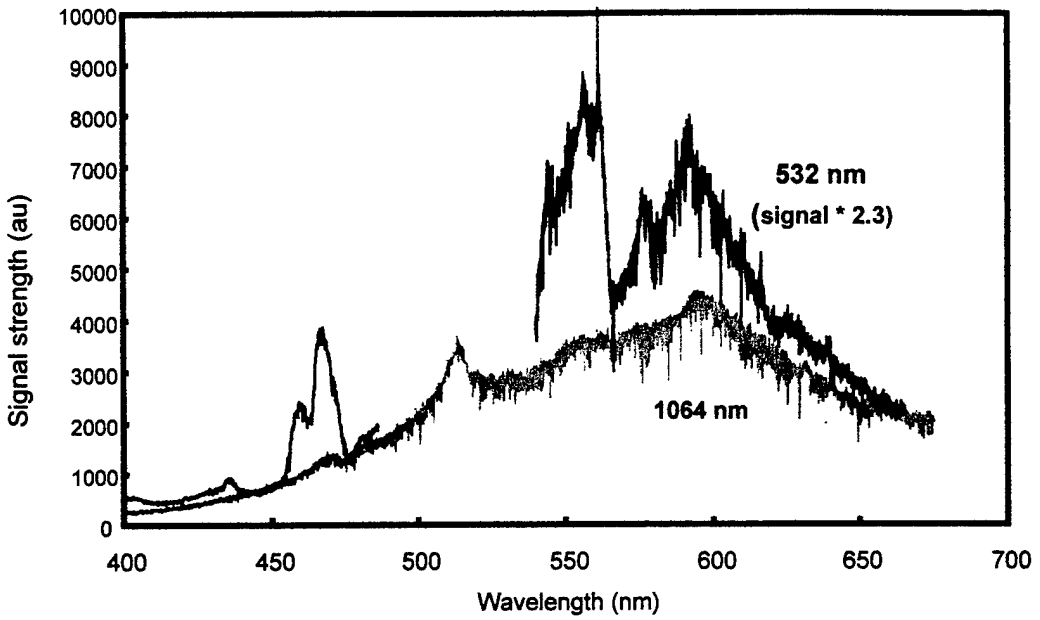


**Figure 19: Experimental measurements of the generation of the $C_2$ emission or Swan bands by 532 nm and 1064 nm laser pulses in a sooting ethylene-air diffusion flame.**

**Particle Sizing**

If particle sizes can be measured, they can be used to help correct the LII measurement for size effects. One method suggested for particle sizing involves measuring the decaying signal during a time when the particle cooling is dominated by conduction to the surrounding gas. Figure 20 shows the signal decay behavior for small and large particles in the first 80 ns after the start of the laser pulse. Since the conduction cooling rate is proportional to the size (or surface area) of the particles but the energy content of the particle scales with its volume, the smallest particles are expected to cool most quickly. Therefore, the smallest particles would exhibit the most rapid signal decay. The model demonstrates this behavior, showing a monotonic dependence on particle size, at least up to 100 nm particles. However, the model also shows that for short measurement times up to about 100 ns after the laser pulse, it would be difficult to discern different signal decay rates for larger particles. This may explain the measurements shown in Figure 12 (page 15) which showed no clear evidence of a particle size effect on cooling rates probably because we used comparatively large soot particles for which the measurement time was too short.

Figure 21 shows the variation in the calibration "constant" C as a function of particle size for conditions that match the experiments shown in Figure 10 on page 14. Based on a 4 μm estimate for the size of the water droplets produced by the nebulizer, there is good agreement between the model and the experiment. The model assumes that the soot particles were solid carbon spheres rather than aggregates so complete correspondence would not be expected; however, the results do suggest that corrections could be applied to the LII signal to account for particle size if the

particle size could be measured, perhaps using the time decay approach suggested by Figure 20. We should also note that for real soot particles, the error in the calibration constant for extended aggregates will depend only on the small spread in primary particle size and would therefore be much less than for the particles formed by the soot generator, say 15-20% or even less.

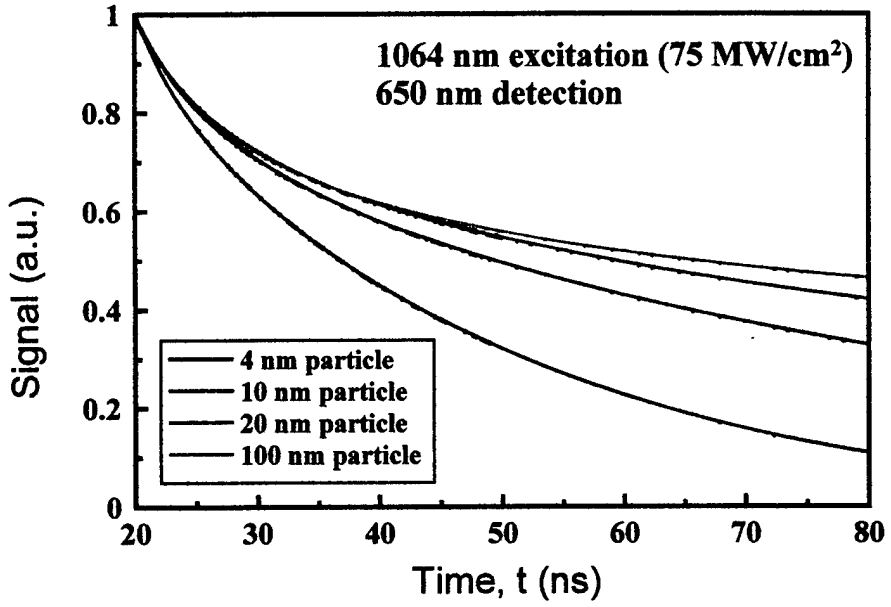


**Figure 20: Predicted decay of the LII signal for various primary particle sizes.**

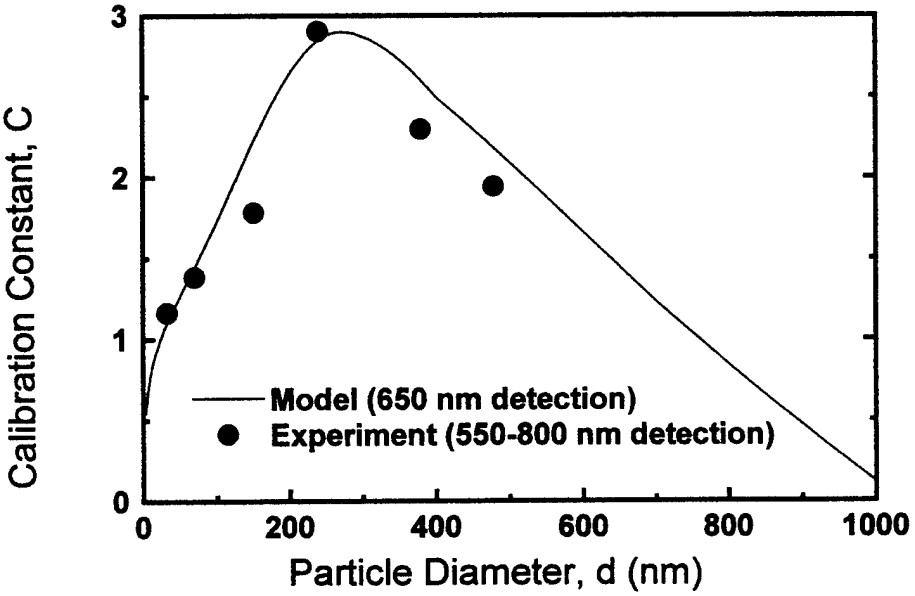


**Figure 21: The relative incandescence signal as a function of particle size; comparison of modeling predictions for detection at 650 nm to the experimental results. The experimental particle sizes are based on a 4 μm estimate of the size of the water droplets produced by the nebulizer, as compared to the 8 μm estimate used in Figure 10.**

## SUMMARY AND CONCLUSIONS

The LII signal was modeled as a function of laser power, soot concentration and particle size. The modeling showed that the signal is expected to be linear with concentration, but will have a particle size dependence because different size particles reach different peak temperatures, and radiate and cool at different rates. The use of laser intensities above a threshold value of about 0.5 J/cm$^2$ (for a 1064 nm Nd:YAG laser) can be used to reduce particle size dependence during the heating phase.

The use of a near infrared laser source is also recommended because it makes it easy to eliminate interference from scattered light by using a detector sensitive to shorter wavelengths. Furthermore, the long wavelength laser does not excite $C_2$ emissions.

Broadband detection in the red part of the spectrum at wavelengths longer than 550 nm provides immunity to background thermal radiation and reduces particle size sensitivity.

Carbon concentration was measured from 8 μg/m$^3$ to nearly 100 mg/m$^3$ in a hot flow. The measurements at 8 μg/m$^3$ were obtained with at least a factor of 10 in sensitivity left in the detector. The measurements were obtained using averages of 128 laser shots, and the 8 μg/m$^3$ data correspond to measurement of as little as $0.16\times10^{-12}$ g of C in the collection volume. Conservatively, as little as $21\times10^{-12}$ g of C could be measured with single laser shot.

The experimental data show that the LII signal is almost linear with soot concentration over more than three orders of magnitude. The measured signals do exhibit a weak dependence on particle morphology and composition. The measurements represent a worst case scenario, with particle size varying from a few tens of nanometers to hundreds of nanometers. Also, the soot particles produced by our generator contain gum residue.

Particle size was not readily determined from the decay rates of the LII signals in the current experiments. This was an unexpected result because theory predicted an effect. The model predicts a monotonic relationship between particle size and decay rate. The reasons for the discrepancy are unclear, but most likely are to do with the unusually large spherical aggregate particle produced by the soot generator. The decay rate of the LII emission from large particles is so slow that the measurements we were able to make over a few hundred nanoseconds were probably insufficient to distinguish between different size particles. The reasonable agreement between the model predictions and the measured size dependence suggests that corrections to the LII signal for particle size effects will be possible.

Experimentally, we found that the temperature of the surrounding gas has little effect on the LII signal, at least for a range of 70-300 °C. This is because the heated soot particles are at a comparatively high temperature of about 4000 K. The result indicates that the technique can be used to measure soot concentration in a hot turbulent exhaust. It also suggests that calibration measurements can be performed under convenient experimental conditions, for example using a soot generator similar to the one employed in these experiments.

## REFERENCES


1 "Soot diagnostics based on laser heating." Lynn A. Melton, Applied Optics. 23, No 13 (1984).

2 "Soot volume fraction and particle size measurements using laser-induced incandescence," B. Mewes, and J.M. Seitzman. Applied Optics 36, (1996).

3 "Spatially resolved measurements of soot volume fraction using laser-induced incandescence." B. Quay, T.W. Lee, T. Ni and R.J. Santoro. Combustion and Flame 97, pp. 384-392 (1994).

4 "Quantitative detection and imaging of soot particles by laser induced incandescence" K.R. McManus, MG Allen, WT Rawlins. 35th Aerospace Sciences Meeting, Jan 6-10, Reno, Nevada. AIAA, Reston VA 22091.

5 "Pulsed photothermal laser deflection for low-level smoke and NO2 measurements in engine exhausts." T.M. Brown, R. W. Pitz, C. F. Hess, and C. P. Wood. Appl. Phys. B, 59, 351-356, 1994.